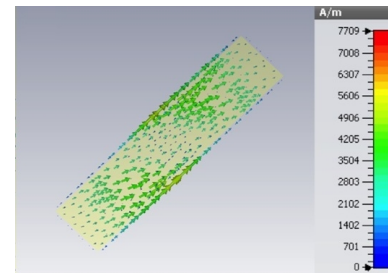




Complementary bilayer metasurfaces for enhanced terahertz wave amplitude and phase manipulation

Dacheng Wang, Yandong Gong and Minghui Hong*

Department of Electrical and Computer Engineering, National University of Singapore, 4 Engineering Drive 3, 117581, Singapore



Abstract: Manipulation of terahertz wave by metasurfaces has shown tremendous potential in developing compact and functional terahertz optical devices. Here, we propose complementary bilayer metasurfaces for enhanced terahertz wave amplitude and phase manipulation. The metasurfaces are composed of one layer of metal cut-wire arrays and one layer of their complementary aperture arrays separated by a dielectric spacer. Through the near-field coupling between transverse magnetic resonances in the metal apertures and electric resonances in the metal cut-wires, the structures can manipulate the cross polarization conversion and phase dispersion of terahertz wave. Particularly, the designed metasurfaces demonstrate a phase delay of 180° between two orthogonal axes with the same transmission amplitude between 0.70 and 1.0 THz, enabling a 45° broadband polarization conversion. When the metal cut-wires are rotated with respect to the apertures or the thickness of the dielectric spacer is changed, the amplitude and phase dispersion of the transmitted terahertz wave can be tuned. Such complementary coupled bilayer metasurfaces offer a new method to control the amplitude and phase dispersion of terahertz wave and promise great potential for applications in terahertz meta-devices.

Keywords: metasurfaces; terahertz; polarization; wave manipulation

DOI: 10.3969/j.issn.1003-501X.2017.01.007

Citation: *Opto-Elec Eng*, 2017, **44**(1): 77–81

1 Introduction

Terahertz wave promises a myriad of fascinating applications in non-destructive testing, sensing, high-speed communication, imaging and security screening^[1-6]. These applications not only call for efficient terahertz emitters and sensitive terahertz detectors, but also demand various functional terahertz optical devices with high performance^[1, 7]. The shortage of these functional devices to control and manipulate terahertz wave has imposed restrictions on the development of terahertz technology. Thus, there is a great research momentum to pursue new approaches for designing terahertz devices that can manipulate terahertz wave flexibly. The main constraint of designing terahertz devices is that limited choices of naturally available materials are capable of interacting with terahertz wave effectively^[8]. Even though the previous works have demonstrated some terahertz

devices through engineering natural materials, these terahertz devices present limited performance to control terahertz wave. For instance, terahertz quarter-wave plates and half-wave plates can be designed using birefringent materials, such as quartz. However, because of the small birefringence index of quartz ($\Delta n = 0.048$ at 1 THz), these devices show millimeter scale thickness with a narrow-band operating frequency^[9]. Multilayer designs can extend the bandwidth, but at the same time the thickness of the devices is increased^[10]. Such issues limit the applications of these devices in the ultra-compact terahertz optical systems.

Over the last decade, metasurfaces, two-dimensional artificial designed meta-atoms, have opened up opportunities to control electromagnetic wave with exotic properties that are unattainable with natural materials, such as negative index, invisible cloaking and hologram^[11-16]. Through tailoring the geometry, size, orientation and material of these meta-atoms in the metasurfaces, prescribed electromagnetic properties can be realized at will. In 2015, Luo, et al. summarized the theory of electromagnetic waves in metasurfaces^[17], which illustrates the

Received 12 October 2016; accepted 10 December, 2016

* E-mail: elehmh@nus.edu.sg

theoretical foundation of metasurfaces. In the optical range, metasurfaces have been applied to many optical systems, such as perfect optical angular momentum generation, vortex generation and dynamic control^[18-20]. Recently, metasurface-based terahertz optical devices have been demonstrated, including filters, modulators, switches, polarizers, wave-plates, perfect absorbers, and lenses^[7-8, 21-26]. The thickness of these meta-devices can be much smaller than the working wavelength, allowing applications in the ultra-compact terahertz systems. However, there are still some obstacles that limit the practical applications of these meta-devices, such as low working efficiency and narrow operating bandwidth. To address these issues, researchers proposed complementary metasurfaces, bilayer metasurfaces, multilayer metasurfaces and active metasurfaces to increase the working efficiency and extend the operating bandwidth^[21, 23, 27-31].

In this work, we propose complementary coupled bilayer metasurfaces to control the amplitude and phase of terahertz wave. The complementary apertures in the metasurfaces give rise to extraordinary optical transmission (EOT)^[26-27]. When metal cut-wires are positioned near the apertures, near-field coupling among the metal wires and their complementary apertures can be applied to manipulate the transmitted amplitude and phase dispersion of terahertz wave. We have demonstrated a broadband polarization conversion by the metasurfaces, in which the polarization of the incident light is rotated by 45° between 0.70 and 1.0 THz. With respect to different relative positions or different thicknesses of the dielectric spacer between the metal wire and its complementary design, the cross-polarization conversion and phase dispersion can be modulated.

2 Design and simulation

The unit cell of the designed complementary bilayer metasurfaces is shown in Fig. 1. As can be seen, the structures consist of two layers of metal resonators with a period of $P = 200 \mu\text{m}$. The unit cell of the first layer is a metal aperture with the length of $l = 175 \mu\text{m}$ and the

width of $w = 40 \mu\text{m}$. The longitudinal direction of the aperture is along x -axis as shown in Fig. 1(a). The unit cell of the second layer is a metal cut-wire with the length of $l = 175 \mu\text{m}$ and the width of $w = 40 \mu\text{m}$. The longitudinal direction of the cut-wire is at $\theta = 45^\circ$ to x -axis as shown in Fig. 1(b). These two layers are separated by a dielectric spacer with a thickness of $t = 8 \mu\text{m}$ as shown in Fig. 1(c). The thickness of the metal film in the two layers is 200 nm. The designed bilayer metasurfaces are simulated using CST microwave studio. The metal film is modeled as a lossy metal with an electrical conductivity of $\sigma = 5.8 \times 10^7 \text{ S/m}$, which can be realized using copper^[22]. The spacer is treated as a lossless dielectric with a permittivity of $\epsilon_1 = 2.9$, which can be realized using terahertz transparent polymers^[32]. A $100 \mu\text{m}$ thick lossless dielectric substrate with a permittivity of $\epsilon_2 = 3.19$ is considered in the simulation to support the first-layer structures for practical realization^[26]. The incident light polarized along y -axis is normally illuminated on the metal apertures as shown in Fig. 1(c). A frequency domain solver with a unit cell boundary condition is applied during the simulation.

The simulated transmission spectra and phase delay of the bilayer metasurfaces are shown in Fig. 2. It is observed that when a y -axis linearly polarized terahertz wave interacts with the metasurfaces, the transmitted terahertz wave contains both co-polarized and cross-polarized light along y - and x -axes, which are marked as T_{yy} and T_{xy} . From Fig. 2(a), we can see that the transmitted terahertz wave shows the same transmission amplitude along y - and x -axes between 0.70 and 1.0 THz with a transmission peak at 0.80 THz, while the phase delay between y - and x -axes is 180° as shown in Fig. 2(b). This means that the output terahertz wave is linearly polarized at 135° to x -axis. Thus, we obtain a polarization rotator that is capable of rotating the polarization of the incident light by 45° based on the bilayer metasurfaces. Meanwhile, a transmission peak at 0.25 THz can be observed for the co-polarized light. This peak corresponds to the EOT effect in the metal apertures. A small peak for cross-polarized light at 0.25 THz can be seen in Fig. 2(a), which corresponds to a weak excitation of the dipole

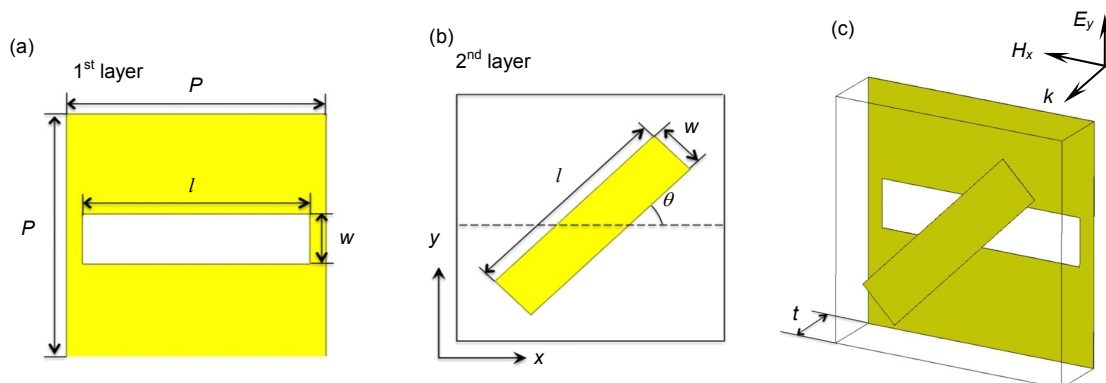


Fig. 1 Schematic of the designed unit cell of (a) the first layer, (b) the second layer and (c) the complementary coupled bilayer metasurfaces.

resonance in the metal cut-wires. A detailed analysis of the resonance modes will be presented in the next discussion section. Compared with those single-layer metasurfaces, the main advantage of the designed bilayer metasurfaces is that they demonstrate a large phase control range over a broadband. As discussed in our previous work, for a simple dipole resonance, it can only present a maximum 180° phase change^[26]. When multiple resonances are designed in the single-layer metasurfaces, the phase delay along different directions would always be smaller than 180° ^[23, 26]. The operating bandwidth is another issue for the single-layer design. However, bilayer metasurfaces can enhance the phase control range and extend the operating bandwidth through the interaction among different layers^[28-29, 31]. In our design, the bilayer metasurfaces show a broadband cross-polarization conversion with a phase delay of 180° , which is hard to be obtained in the single-layer metasurfaces.

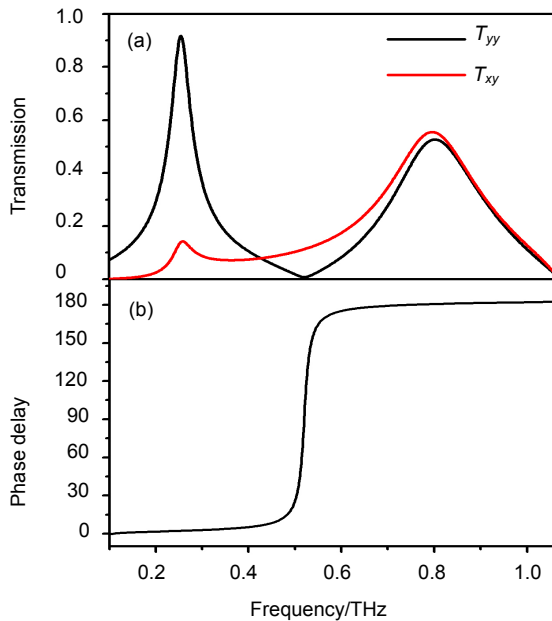


Fig. 2 Transmission spectra (a) for the co-polarized and the cross-polarized light with (b) the phase delay.

3 Analysis

In order to elucidate the resonance modes and their near-field interaction in the designed bilayer metasurfaces, surface current distributions at the resonances are simulated. Fig. 3(a) shows the surface current distribution in the metal apertures at 0.25 THz, which indicates the excitation of the transverse magnetic dipole resonance in the apertures. The resonance in the aperture gives rise to the EOT effect and presents a transmission peak for the co-polarized light at 0.25 THz. The surface current distribution in the metal cut-wires is shown in

Fig. 3(b). It is observed that the electric dipole resonance is excited, which results in the cross-polarized transmission peak at 0.25 THz. Figs. 3(c) and 3(d) provide the surface current distributions of the metal apertures and cut-wires at 0.80 THz. From these two figures, we can observe that surface current distributions in these two layers show opposite directions, indicating that a magnetic dipole can be formed within the circulating currents between the aperture and the cut-wire. The strong coupling between these two layers leads to the transmission peak at 0.80 THz. Furthermore, the phase dispersion of the transmitted light is modified by this coupling effect and a phase delay of 180° between 0.70 and 1.0 THz is achieved. Therefore, a broadband polarization conversion is realized by the complementary coupled bilayer metasurfaces.

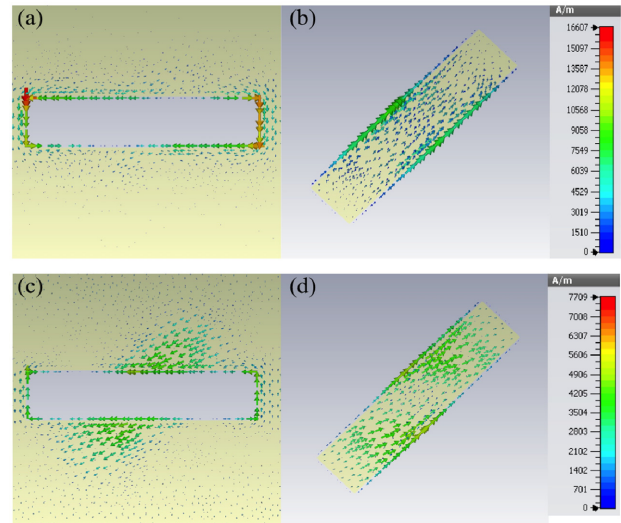


Fig. 3 Surface current distributions of (a) the metal aperture and (b) metal cut-wire at 0.25 THz. Surface current distributions of (c) the metal aperture and (d) the metal cut-wire at 0.80 THz.

To further investigate the coupling effect in the bilayer metasurfaces, different relative rotation angles between the aperture and the cut-wire and different thicknesses of the dielectric spacer are simulated. When the rotation angle changes from 0° to 15° , 30° , 45° , 60° , 75° and 90° , the simulated co-polarized and cross-polarized transmission amplitudes are shown in Figs. 4(a) and 4(b) with the phase delay shown in Fig. 4(c). When the rotation angle is 0° , a transmission peak for the co-polarized light can be observed at 0.43 THz, which corresponds to the dipole resonance in the metal apertures. No cross-polarized component can be obtained, which indicates that there is no coupling between the aperture and the cut-wire. When the rotation angle is 15° , two transmission peaks at 0.33 and 0.60 THz for the co-polarized light can be observed. Meanwhile, the cross-polarized light presents two transmission peaks at 0.34 and 0.58 THz. These four transmission peaks indicate a strong coupling between

the metal aperture and the metal cut-wire. When the rotation angle further increases, the high frequency resonances for both the co-polarized and cross-polarized light shift to a higher frequency, while the low frequency resonances for both the co-polarized and cross-polarized light shift to a lower frequency. The phase delay between the co-polarized and cross-polarized light is shown in Fig. 4(c). As can be seen, when the rotation angle changes, the phase delays maintain 180° in a broadband with a small shift of the frequency. The phase delays for the rotation angles of 0° and 90° are not provided since no cross-polarization light is obtained in these two cases. Therefore, the rotation angle between the metal aperture and the metal cut-wire changes the resonance frequency for both the co-polarized and cross-polarized light with a similar phase delay.

Besides the rotation angle, the thickness of the dielectric spacer between the metal aperture and the cut-wire is studied to tune the coupling effect in the bilayer metasurfaces. Fig. 5(a) and 5(b) show the transmission spectra of the co-polarized and cross-polarized light when the thickness of the dielectric spacer changes from 1 to 2, 4, 8,

15, 20 and $30\ \mu\text{m}$. It is observed from Fig. 5(a) that when the thickness of the dielectric spacer increases, the resonance frequency of the metal aperture decreases, while the frequency of the coupled magnetic dipole resonance increases. A similar frequency variation trend can be seen in Fig. 5(b) for the cross-polarized light. Furthermore, when the thickness of the dielectric spacer is smaller, a larger transmission peak for the cross-polarized light is achieved. This indicates that a thinner dielectric spacer would provide a stronger coupling between the aperture and the cut-wire. The phase delays with respect to different thicknesses of the dielectric spacer are shown in Fig. 5(c). As can be seen, with a thinner dielectric spacer, a broader bandwidth for the phase delay of 180° can be realized. Thus, the thickness of the dielectric spacer modifies the coupling effect in the bilayer metasurfaces, enabling a high efficiency cross-polarization conversion and a broadband phase delay.

4 Conclusions

In summary, we proposed complementary coupled bi-

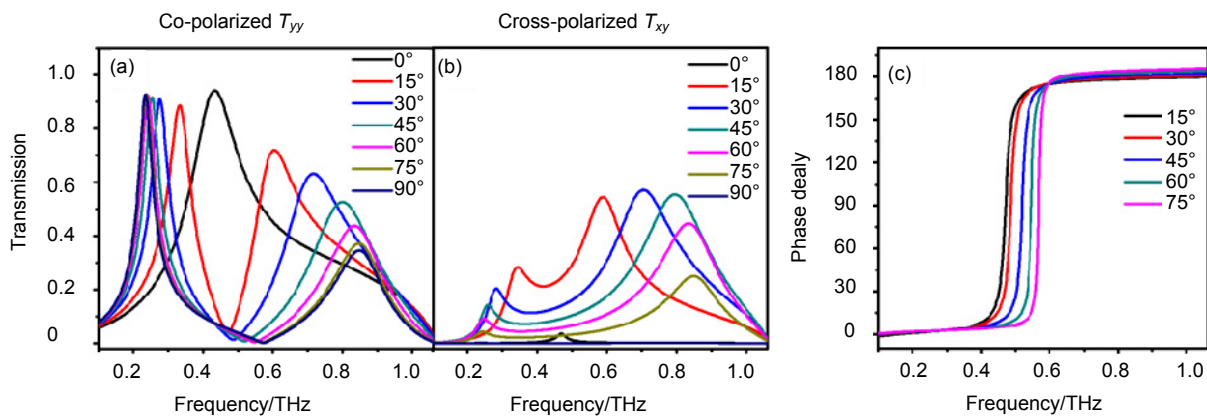


Fig. 4 Transmission spectra for (a) the co-polarized and (b) cross-polarized light when the rotation angle θ changes from 0° to 15° , 30° , 45° , 60° , 75° and 90° . (c) Phase delay between the co-polarized and cross-polarized light.

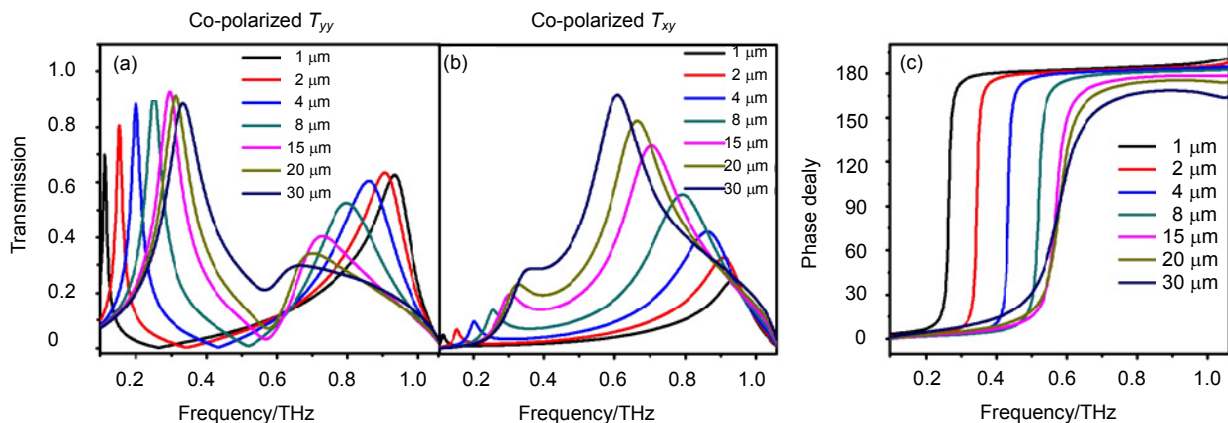


Fig. 5 Transmission spectra for (a) the co-polarized and (b) cross-polarized light when the thickness of the dielectric spacer varies from 1 to 2, 4, 8, 15, 20 and $30\ \mu\text{m}$. (c) Phase delay between the co-polarized and cross-polarized light.

layer metasurfaces to manipulate the amplitude and phase dispersion of terahertz wave. The proposed bilayer metasurfaces are composed of metal apertures with their complementary wires separated by a dielectric spacer. The coupling between the transverse magnetic dipole resonance in the metal aperture and the electric dipole resonance in the metal wire can be applied to manipulate the cross-polarization conversion and phase dispersion of terahertz wave. We have demonstrated a 45° polarization rotation based on the bilayer metasurfaces between 0.70 and 1.0 THz. With respect to different rotation angles between the aperture and the cut-wire or different thicknesses of the dielectric spacer, the transmission amplitude and phase delay can be tuned. The proposed complementary bilayer metasurfaces provide a new method to control terahertz wave and can be applied to design high-performance terahertz meta-devices.

Acknowledgements

This research is supported in part by the National Research Foundation, Prime Minister's Office, Singapore under its Competitive Research Program (CRP Award No. NRF-CRP10-2012-04) and in part by EDB, Singapore with grant No. S15-1322-IAF OSTIn-SIAG.

References

- 1 Tonouchi M. Cutting-edge terahertz technology [J]. *Nature Photonics*, 2007, **1**(2): 97–105.
- 2 Choi Y, Choi J W, Cioffi J M. A geometric-statistic channel model for THz indoor communications[J]. *Journal of Infrared, Millimeter, and Terahertz Waves*, 2013, **34**(7/8): 456–467.
- 3 Federici J F, Schulkin B, Huang Feng, *et al.* THz imaging and sensing for security applications—explosives, weapons and drugs[J]. *Semiconductor Science and Technology*, 2005, **20**(7): S266–S280.
- 4 Hasebe T, Kawabe S, Matsui H, *et al.* Metallic mesh-based terahertz biosensing of single- and double-stranded DNA[J]. *Journal of Applied Physics*, 2012, **112**(9): 094702.
- 5 Orlando A R, Gallerano G P. Terahertz radiation effects and biological applications[J]. *Journal of Infrared, Millimeter, and Terahertz Waves*, 2009, **30**(12): 1308–1318.
- 6 Wojdyla A, Gallot G. Attenuated internal reflection terahertz imaging[J]. *Optics Letters*, 2013, **38**(2): 112–114.
- 7 Chen H T, Padilla W J, Cich M J, *et al.* A metamaterial solid-state terahertz phase modulator[J]. *Nature Photonics*, 2009, **3**(3): 148–151.
- 8 Chen Houtong, Padilla W J, Zide J M O, *et al.* Active terahertz metamaterial devices[J]. *Nature*, 2006, **444**(7119): 597–600.
- 9 Masson J B, Gallot G. Terahertz achromatic quarter-wave plate[J]. *Optics Letters*, 2006, **31**(2): 265–267.
- 10 Chen Zaichun, Gong Yandong, Dong Hui, *et al.* Terahertz achromatic quarter wave plate: design, fabrication, and characterization[J]. *Optics Communications*, 2014, **311**: 1–5.
- 11 Yu Nanfang, Capasso F. Flat optics with designer metasurfaces [J]. *Nature Materials*, 2014, **13**(2): 139–150.
- 12 Zheng Guoxing, Mühlenbernd H, Kenney M, *et al.* Metasurface holograms reaching 80% efficiency[J]. *Nature Nanotechnology*, 2015, **10**(4): 308–312.
- 13 Kildishev A V, Boltasseva A, Shalaev V M. Planar photonics with metasurfaces[J]. *Science*, 2013, **339**(6125): 1232009.
- 14 Zheludev N I, Kivshar Y S. From metamaterials to metadevices [J]. *Nature Materials*, 2012, **11**(11): 917–924.
- 15 Meinzer N, Barnes W L, Hooper I R. Plasmonic meta-atoms and metasurfaces[J]. *Nature Photonics*, 2014, **8**(12): 889–898.
- 16 Lin Dianmin, Fan Pengyu, Hasman E, *et al.* Dielectric gradient metasurface optical elements[J]. *Science*, 2014, **345**(6194): 298–302.
- 17 Luo Xiangang. Principles of electromagnetic waves in metasurfaces[J]. *Science China Physics, Mechanics & Astronomy*, 2015, **58**(9): 594201.
- 18 Pu Mingbo, Li Xiong, Ma Xiaoliang, *et al.* Catenary optics for achromatic generation of perfect optical angular momentum[J]. *Science Advances*, 2015, **1**(9): e1500396.
- 19 Ma Xiaoliang, Pu Mingbo, Li Xiong, *et al.* A planar chiral metasurface for optical vortex generation and focusing[J]. *Scientific Reports*, 2015, **5**: 10365.
- 20 Li Xiong, Pu Mingbo, Wang Yanqin, *et al.* Dynamic control of the extraordinary optical scattering in semicontinuous 2D metamaterials[J]. *Advanced Optical Materials*, 2016, **4**(5): 659–663.
- 21 Cong Longqing, Cao Wei, Zhang Xueqian, *et al.* A perfect metamaterial polarization rotator[J]. *Applied Physics Letters*, 2013, **103**(17): 171107.
- 22 Gao Lihua, Cheng Qiang, Yang Jing, *et al.* Broadband diffusion of terahertz waves by multi-bit coding metasurfaces[J]. *Light: Science & Applications*, 2015, **4**(9): e324.
- 23 Wang Dacheng, Zhang Lingchao, Gu Yinghong, *et al.* Switchable ultrathin quarter-wave plate in terahertz using active phase-change metasurface[J]. *Scientific Reports*, 2015, **5**: 15020.
- 24 Wang Dacheng, Qiu Chengwei, Hong Minghui. Coupling effect of spiral-shaped terahertz metamaterials for tunable electromagnetic response[J]. *Applied Physics A*, 2014, **115**(1): 25–29.
- 25 Jia Shengli, Wan Xiang, Bao Di, *et al.* Independent controls of orthogonally polarized transmitted waves using a Huygens metasurface[J]. *Laser & Photonics Review*, 2015, **9**(5): 545–553.
- 26 Wang Dacheng, Gu Yinghong, Gong Yandong, *et al.* An ultrathin terahertz quarter-wave plate using planar babinet-inverted metasurface[J]. *Optics Express*, 2015, **23**(9): 11114–11122.
- 27 Zalkovskij M, Malureanu R, Kremers C, *et al.* Optically active Babinet planar metamaterial film for terahertz polarization manipulation[J]. *Laser & Photonics Review*, 2013, **7**(5): 810–817.
- 28 Qin Fei, Ding Lu, Zhang Lei, *et al.* Hybrid bilayer plasmonic metasurface efficiently manipulates visible light[J]. *Science Advance*, 2016, **2**(1): e1501168.
- 29 Grady N K, Heyes J E, Chowdhury D R, *et al.* Terahertz metamaterials for linear polarization conversion and anomalous refraction[J]. *Science*, 2013, **340**(6138): 1304–1307.
- 30 Chen W C, Landy N I, Kempa K, *et al.* A subwavelength extraordinary-optical-transmission channel in babinet metamaterials [J]. *Advanced Optical Materials*, 2013, **1**(3): 221–226.
- 31 Cong Longqing, Xu Ningning, Gu Jianqiang, *et al.* Highly flexible broadband terahertz metamaterial quarter-wave plate[J]. *Laser & Photonics Review*, 2014, **8**(4): 626–632.
- 32 Grbovic D, Alves F, Kearney B, *et al.* Metal-organic hybrid resonant terahertz absorbers with SU-8 photoresist dielectric layer [J]. *Journal of Micro/Nanolithography, MEMS and MOEMS*, 2013, **12**(4): 041204.